Copper(II) Chemistry in Hexaaza Binucleating Macrocycles: Hydroxide and Acetate Derivatives

Peter K. Coughlin[1a] and Stephen J. Lippard*[1a,b]

Contribution from the Departments of Chemistry, Columbia University, New York, New York 10027, and the Massachusetts Institute of Technology, Cambridge, Massachusetts 02139. *Received August 25, 1983*

Abstract: This article reports the synthesis, structures, magnetic properties, and solution stability of compounds formed when $\{Cu_2 \subset A\}^{4+}$, A = 1,4,7,13,16,19-hexaaza-10,22-dioxacyclotetracosane, reacts with the simple anions OH^- and $CH_3CO_2^-$ (OAc). Hydroxide ion forms a bridged binuclear complex, the structure of which was revealed by X-ray analysis of single crystals of $[Cu_2(OH)(ClO_4) \subset A](ClO_4)_2 \cdot CHCl_3$. The ($\mu$-hydroxo)dicopper(II) unit is characterized by short Cu–O bond lengths of 1.912 (4) and 1.922 (4) Å and a Cu–OH–Cu angle of 143.6 (2)°. Although the hydroxyl proton was not located crystallographically, its presence was confirmed by infrared spectroscopic studies on the deuterated form of the complex. The geometry around the copper atoms is distorted square pyramidal with the basal plane positions occupied by the amine nitrogen atoms and hydroxide oxygen atom and the apical position by a weakly bonded oxygen atom of a bridging perchlorate group (Cu–$OClO_3$, 2.540 (8) and 2.568 (8) Å). Temperature-dependent magnetic susceptibility studies revealed strong antiferromagnetic coupling with $J = -496$ (7) cm^{-1}. Optical spectroscopic examination of aqueous solutions of the complex showed it to be stable over the range $6 < pH < 11$. A 330-nm optical band was found to be perchlorate ion dependent. These results are discussed with reference to binuclear copper centers in biology. The structure of the crystalline acetate derivative, $[Cu_2(OAc)_2A](ClO_4)_2$, was found by X-ray diffraction to be a linear polymer propagated by acetate-bridged dicopper(II) centers and the macrocycle A. The acetate groups in the binuclear $\{Cu_2(OAc)_2\}^{2+}$ moiety have a syn–anti conformation and link the copper atoms (Cu···Cu, 5.23 Å) through basal and apical positions of a square-pyramidal structure. As a consequence, the copper(II) centers are only very weakly antiferromagnetically coupled ($J \sim -1$ cm^{-1}). This result contrasts markedly with the magnetic behavior of copper acetate in which the syn–syn bridge conformation produces a short Cu···Cu contact and strong antiferromagnetic coupling. Recrystallization of the acetate compound gave the more stable hydroxide-bridged complex. The ligand A is shown to adopt "planar", "U-shaped", and "S-shaped" geometries depending upon the conformational preferences of its bridged bimetallic center.

Recently we have explored the chemistry of the imidazolate-bridged dicopper(II) ion in binucleating macrocycles A and A′ to gain insight into the active site of bovine erythrocyte superoxide

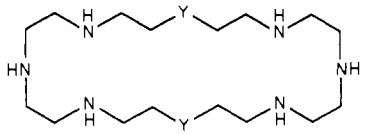

macrocycle A, Y = O
macrocycle A', Y = CH_2

dismutase and its derivatives.[2,3] Because of the widespread occurrence of binuclear copper centers in biology,[4] it was of interest to extend these studies more generally to include potentially bridging ligands other than imidazolate. Since the stability of the $Cu_2(im)^{3+}$ (imH = imidazole) ion is markedly enhanced by

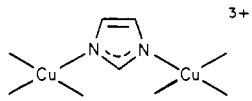

incorporation into A and A′,[2d,5] bridging ligands congruent with fragments of the imidazolate ion were investigated, viz.

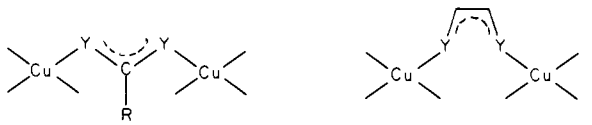

Examples of such ligands include acetate, catecholate, and carbonate. Also studied were single-atom bridging ligands such as halide, alkoxide, aryloxide, and hydroxide, which are especially interesting since a single-atom bridge most likely links the oxidized copper centers in hemocyanin, tyrosinase, and related proteins.[4]

In this paper we describe the reaction of $\{Cu_2 \subset A\}^{3+}$ with hydroxide and acetate anions. As reported in preliminary forms,[6] the hydroxide-bridged dicopper(II) complex $[Cu_2(OH)(ClO_4) \subset A]^{2+}$ has magnetic and spectroscopic properties that closely mimic those characteristic of binuclear copper centers in biology. Subsequent potentiometric equilibrium titrations underscored the stability of the $[Cu_2(OH) \subset A]^{3+}$ ion in solution,[5] and a variety of related monohydroxo-bridged dicopper(II) complexes have recently been described.[7] In addition to providing further details about the physical and chemical properties of the hydroxide-bridged complex, including an improved synthesis, the present article reports the synthesis, structure, and magnetic properties of an unusual acetate-bridged polymer. An analysis of the conformational properties of the ligand A is also presented.

Experimental Section

Synthesis. Macrocycle A, 1,4,7,13,16,19-hexaaza-10,22-dioxacyclotetracosane, prepared as described previously,[2a] was a gift from Professor J.-M. Lehn. All other materials were commercially available and used without further purification. Solution electronic spectra were recorded with a Cary-118C spectrophotometer using 1-cm path length quartz cells.

* Address correspondence to this author at M.I.T.

(1) (a) Columbia University. (b) Massachusetts Institute of Technology.
(2) (a) Coughlin, P. K.; Dewan, J. C.; Lippard, S. J.; Watanabe, E.-i.; Lehn, J.-M. *J. Am. Chem. Soc.* **1979**, *101*, 265. (b) Coughlin, P. K.; Lippard, S. J.; Martin, A. E.; Bulkowski, J. E. *Ibid.* **1980**, *102*, 7616. (c) Coughlin, P. K.; Martin, A. E.; Dewan, J. C.; Watanabe, E.-i.; Bulkowski, J. E.; Lehn, J.-M.; Lippard, S. J. *Inorg. Chem.*, in press. (d) Coughlin, P. K.; Lippard, S. J. *Ibid.*, in press.
(3) Strothkamp, K. G.; Lippard, S. J. *Acc. Chem. Res.* **1982**, *10*, 318.
(4) Solomon, E. I. In "Copper Proteins"; Spiro, T. G., Ed.; Wiley: New York, 1981, p 41 and references cited therein.
(5) Motekaitis, R. J.; Martell, A. E.; Lecomte, J.-P.; Lehn, J.-M. *Inorg. Chem.* **1983**, *22*, 609.
(6) Coughlin, P. K.; Lippard, S. J. *J. Am. Chem. Soc.* **1981**, *103*, 3228.
(7) (a) Haddad, M. S.; Wilson, S. R.; Hodgson, D. J.; Hendrickson, D. N. *J. Am. Chem. Soc.* **1981**, *103*, 384. (b) Haddad, M. S.; Hendrickson, D. N. *Inorg. Chim. Acta* **1978**, *28*, L121–L122. (c) Burk, P. L.; Osborn, J. A.; Youinou, M.-T.; Agnus, Y.; Louis, R.; Weiss, R. *J. Am. Chem. Soc.* **1981**, *103*, 1273. (d) Drew, M. G. B.; McCann, M.; Nelson, S. M. *J. Chem. Soc., Dalton Trans.* **1981**, 1868. (e) Drew, M. G. B.; Nelson, J.; Esho, F.; McKee, V.; Nelson, S. M. *Ibid.* **1982**, 1837.

0002-7863/84/1506-2328$01.50/0

Nujol mull infrared spectra were recorded with a Perkin-Elmer Model 621 grating infrared spectrophotometer. The wavelength was calibrated at numerous points in each spectrum with polystyrene film.

$[Cu_2(OH)(ClO_4)\subset A](ClO_4)_2\cdot CHCl_3$ (1). To 3.0 mL of a stirred 29 mM methanolic solution of macrocycle A (87 μmol) was added dropwise a solution of $Cu(ClO_4)_2\cdot 6H_2O$ (64 mg, 173 μmol) in 3.0 mL of methanol. To the resulting dark blue solution was added 87 μL of 1.0 N aqueous sodium hydroxide as stirring continued for 5 min. If this compound was made in more concentrated soluton, a precipitate formed which had to be redissolved by adding water. Maximum yields and shortest crystallization times were attained when no precipitate formed at this point. Vapor diffusion of chloroform into the solution gave crystals of $[Cu_2(OH)(ClO_4)\subset A](ClO_4)_2\cdot CHCl_3$ in 85% yield.

Anal. Calcd for $[Cu_2(OH)(ClO_4)\subset A](ClO_4)_2\cdot CHCl_3$; $Cu_2C_{17}H_{40}N_6O_{15}Cl_6$: C, 22.48; H, 4.44; N, 9.25; Cl, 23.42. Found: C, 22.68; H, 4.62; N, 9.39; Cl, 24.15. Infrared spectrum: N–H stretches, 3288, 3264 cm^{-1}; O–H stretch, 3472 cm^{-1}. Optical spectrum (aqueous solution): λ_{max} (ϵ, M^{-1} cm^{-1}) 637 (240), 330 (1800, sh), 265 (9300) nm.

The deuterated compound $[Cu_2(OD)(ClO_4)\subset A](ClO_4)_2\cdot CHCl_3$ was made in an analogous manner except that the original 29 mM solution of macrocycle A in methanol was diluted in half with methanol-d_1, CH_3OD; the solvent was removed under vacuum and restored to 29 mM in macrocycle with methanol-d_1. In the rest of the synthesis methanol-d_1 was used instead of methanol, and 1.81 N sodium deuteroxide in D_2O was used instead of aqueous sodium hydroxide. The synthesis was run at $^1/_3$ the scale and the yield was 80%. Infrared spectrum: similar to $[Cu_2(OH)(ClO_4)\subset A](ClO_4)_2\cdot CHCl_3$ except N–D stretches, 2438, 2412 cm^{-1}; O–D stretch 2560 cm^{-1}.

$[Cu_2(OH)(ClO_4)\subset A](ClO_4)_2\cdot CHCl_3$ was also obtained from other sources of base. The use of 0.5 N (aqueous) sodium carbonate solution as the source of base in the stoichiometry of 1 carbonate per 2 equiv of copper followed by vapor diffusion of chloroform gave small crystals of an unknown compound. From the rapidly released gas when dissolved in acid this material was assumed to contain carbonate. The unit cell of this crystalline complex was found to be monoclinic with a = 11.90 Å, b = 39.84 Å, c = 12.04 Å, and β = 113.5°, and further studies are in progress. When the complex was recrystallized from warm methanol with use of vapor diffusion of chloroform, the compound $[Cu_2(OH)(ClO_4)\subset A](ClO_4)_2\cdot CHCl_3$ was obtained. A similar transformation occurred when methanolic sodium acetate was used as the source of base. Vapor diffusion of chloroform into the original reaction mixture gave a microcrystalline material that could be recrystallized either from methanol with vapor diffusion of chloroform to give the hydroxo-bridged compound, identified by X-ray diffraction, or from excess methanolic acetate to give an acetate-bridged polymer, discussed below.

$[Cu_2(O_2CCH_3)_2A]_n(ClO_4)_{2n}$ (2). To 3.0 mL of a stirred 29 mM methanolic solution of macrocycle A was added dropwise 2.0 mL of a methanolic solution of $Cu(ClO_4)_2\cdot 6H_2O$ (64 mg, 173 μmol). While stirring continued, 173 μL of 0.5 N methanolic sodium acetate was added. Vapor diffusion of chloroform into this reaction mixture gave small blue crystals. The crystals were redissolved in a methanolic solution of 0.5 N sodium acetate and 0.5 N acetic acid. Vapor diffusion of benzene into this solution gave single crystals of $[Cu_2(O_2CCH_3)_2A]_n(ClO_4)_{2n}$, identified by X-ray crystallographic methods.

Magnetic Susceptibility Measurements. The magnetic susceptibilities of $[Cu_2(OH)(ClO_4)\subset A](ClO_4)_2\cdot CHCl_3$ and $[Cu_2(OAc)_2A]_n(ClO_4)_{2n}$ were measured over the temperature range $4.2 < T < 300$ K by the Faraday method using a locally constructed susceptometer. The details of the construction and calibration of the susceptometer are described elsewhere.[8] Data for the hydroxide-bridged complex at temperatures less than 150 K showed only a slight, ~1%, paramagnetic impurity and were not used further in the analysis. The remaining data were fit to the Bleaney–Bowers equation[9] as described previously for related studied in our laboratory.[2d] The percent impurity was set to 1% and g was assigned as the ESR-measured value of 2.09; neither of these parameters was refined. The only parameters varied were the coupling constant and a small diamagnetic correction used to eliminate systematic errors. The acetate compound was fit to the Curie–Weiss law by the method of least-squares using a locally written program that allowed both C and θ to refine.[2d]

X-ray Data Collection and Reduction. $[Cu_2(OH)(ClO_4)\subset A](ClO_4)_2\cdot CHCl_3$ (1). The crystals obtained by vapor diffusion grew as clusters. A single crystal suitable for X-ray study was obtained from a batch in which sodium acetate was used as the source of base by cleaving one of the clusters with a razor blade. The crystal was bounded by (010) and (0$\bar{1}$0), 0.24 mm apart, (10$\bar{1}$) and ($\bar{1}$01), 0.50 mm apart, (111), 0.05 mm from a central point, and the cleaved face (2$\bar{1}\bar{2}$), 0.16 mm from a central point. Preliminary precession and Weissenberg photographs using Cu Kα radiation (λ 1.5418 Å) showed the space group to be $P2_1/c$ (C_{2h}^5, No. 14).[10] The photographs also showed additional pseudomirror symmetry and systematic weaknesses, which, except for the fact that $\beta \neq 90°$, resembled photographs of an orthorhombic cell, indicating possible pseudosymmetry in the cell. A systematic search using TRACER-II failed to reveal any symmetry higher than monoclinic primative. This pseudosymmetry and the related orthorhombic space group are further discussed below. The quality of the crystal was examined and found to be acceptable by taking open-counter ω scans of several strong, low-angle reflections ($\Delta\omega_{1/2} \sim 0.15°$). Further details of the data colleciton and reduction are given in Table I.

Table I. Experimental Details of the X-ray Diffraction Studies of $[Cu_2(OH)(ClO_4)\subset A](ClO_4)_2\cdot CHCl_3$ (1) and $[Cu_2(OAc)_2A]_n(ClO_4)_{2n}$ (2)

(A) Crystal Parameters[a] at 26 °C

compd no.	1	2	compd no.	1	2
a, Å	14.487 (2)	8.5065 (13)	space group	$P2_1/c$	$P2_1/n$
b, Å	15.282 (2)	10.417 (2)	Z	4	2
c, Å	15.573 (2)	17.653 (3)	ρ(calcd), g cm^{-3}	1.751	1.700
β, deg	91.79 (1)	99.18 (1)	ρ(obsd),[b] g cm^{-3}	1.754 (2)	1.694 (4)
V, Å^3	3445.9	1544.3	mol wt	908.4	790.6

(B) Measurement of Intensity Data[c]

instrument: Enraf-Nonius CAD-4F κ-geometry diffractometer
radiation: Mo Kα ($\lambda_{\bar{\alpha}}$ 0.710 73 Å) graphite monochromatized

compd no.	1	2
standards,[d] measured	($\bar{1}$1$\bar{7}$)	($\bar{1}$5$\bar{8}$)
every 1 h of X-ray	(7$\bar{3}$6)	(05$\bar{3}$)
exposure time	(8$\bar{3}$1)	($\bar{2}$42)
range of refls collected	[3 ≤ 2θ ≤ 50°-(±h,+k,+l)]	[3 ≤ 2θ ≤ 55°-(+h,+k,±l)]

(C) Treatment of Intensity Data[e]

compd no.	1	2
μ, cm^{-1}	17.8	16.3
transmission factor range[f]	0.61–0.74	0.59–0.77
averaging, R_{av}[c]	0.042	0.062
no. of reflections after averaging	6066	3524
obsd unique data $F_o > 4\sigma(F_o)$	4305	2051

[a] From a least-squares fit of the setting angles of 25 reflections with $2\theta > 30°$. [b] By neutral buoyancy in a mixture of $CHBr_3$ and $CHCl_3$. [c] See Silverman et al. [Silverman, L. D.; Dewan, J. C.; Giandomenico, C. M.; Lippard, S. J. *Inorg. Chem.* 1980, *19*, 3379] for typical data collection and reduction procedures employed in our laboratory. [d] Used to scale the data for anisotropic decay; ~12% for 1 and 5% for 2. [e] F_o and $\sigma(F_o)$ were corrected for background, attenuator, and Lorentz-polarization of X-radiation as described in the reference of footnote *c*.

$[Cu_2(OAc)_2A]_n(ClO_4)_{2n}$ (2). Crystals obtained by vapor diffusion of benzene into methanolic solutions of **2** were suitable for single-crystal X-ray study. A plate bounded by (101) and ($\bar{1}$0$\bar{1}$), 0.13 mm apart, (010) and (0$\bar{1}$0), 0.35 mm apart, and (001) and (00$\bar{1}$), 0.28 mm apart was used for the structure determination. Preliminary inspection of the diffraction data indicated the space group to be $P2_1/n$, (C_{2h}^5, No. 14).[10] This cell was used instead of the conventional $P2_1/c$ choice because the β angle was closer to 90°. Details of the data collection and reduction are given in Table I.

Structure Solution and Refinement. Compound 1. The structure was solved by heavy-atom methods and refined by using anisotropic thermal parameters for all non-hydrogen atoms.[11] Neutral-atom scattering factors for the non-hydrogen atoms and corrections for anomalous dispersion effects for copper and chlorine atoms were taken from ref 12.

(8) Coughlin, P. K. Ph.D. Dissertation, Columbia University, 1981.
(9) Bleaney, B.; Bowers, K. D. *Proc. R. Soc. London, Ser. A* **1952**, *214*, 451.
(10) "International Tables for X-ray Crystallography", 3rd ed.; Kynoch Press: Birmingham, England, 1973; Vol. I, p 99.
(11) All calculations were performed on a DEC VAX-11/780 computer using SHELX-76: Sheldrick, G. M. In "Computing in Crystallography"; Schenk, H.; Olthof-Hazekamp, R., van Koningsveld, H.; Bossi, G. C.; Eds.; Delft University Press: Delft, The Netherlands, 1978; pp 34–42. TRACER-II is a lattice transformation cell reduction program by Lawton.
(12) "International Tables for X-ray Crystallography"; Kynoch Press: Birmingham, England, 1974; Vol. IV, pp 99, 149.

Table II. Final Positional Parameters for $[Cu_2(OH)(ClO_4)\subset A](ClO_4)_2 \cdot CHCl_3$ (1)[a]

atom	x	y	z
Cu(1)	0.15871 (4)	−0.07505 (4)	0.18622 (5)
Cu(2)	0.35355 (5)	0.07528 (5)	0.18138 (5)
O(1)	0.2581 (3)	0.0012 (2)	0.2223 (3)
N(1)	0.2297 (3)	−0.1895 (3)	0.2092 (4)
C(2)	0.1796 (5)	−0.2571 (5)	0.1581 (6)
C(3)	0.0768 (5)	−0.2419 (5)	0.1605 (5)
N(4)	0.0610 (4)	−0.1506 (3)	0.1319 (3)
C(5)	−0.0304 (4)	−0.1133 (5)	0.1465 (5)
C(6)	−0.0207 (4)	−0.0152 (5)	0.1369 (5)
N(7)	0.0556 (3)	0.0154 (3)	0.1938 (3)
C(8)	0.0229 (4)	0.0347 (4)	0.2811 (4)
C(9)	0.0988 (4)	0.0693 (4)	0.3401 (4)
O(10)	0.1390 (3)	0.1416 (3)	0.2986 (3)
C(11)	0.2238 (4)	0.1721 (5)	0.3379 (4)
C(12)	0.2682 (5)	0.2319 (4)	0.2745 (5)
N(13)	0.2806 (3)	0.1902 (3)	0.1903 (4)
C(14)	0.3262 (5)	0.2509 (5)	0.1315 (5)
C(15)	0.4275 (5)	0.2396 (5)	0.1380 (5)
N(16)	0.4456 (4)	0.1466 (3)	0.1197 (3)
C(17)	0.5383 (4)	0.1109 (5)	0.1379 (5)
C(18)	0.5306 (4)	0.0128 (4)	0.1372 (5)
N(19)	0.4582 (3)	−0.0148 (3)	0.1964 (3)
C(20)	0.4979 (4)	−0.0313 (4)	0.2840 (4)
C(21)	0.4259 (4)	−0.0562 (4)	0.3455 (4)
O(22)	0.3777 (3)	−0.1299 (3)	0.3114 (3)
C(23)	0.2953 (4)	−0.1538 (5)	0.3543 (4)
C(24)	0.2438 (5)	−0.2186 (4)	0.3005 (5)
Cl(1)[b]	0.2432 (12)	0.0084 (8)	−0.0073 (12)
Cl(1')	0.2548 (11)	−0.0213 (8)	−0.0034 (11)
O(1A)	0.1769 (7)	−0.0334 (10)	0.0297 (5)
O(1B)	0.3309 (5)	0.0119 (8)	0.0294 (4)
O(1C)	0.2473 (4)	−0.0147 (7)	−0.0942 (3)
O(1D)	0.2104 (18)	0.0827 (11)	0.0195 (13)
O(1D')	0.296 (2)	−0.0913 (15)	0.0350 (16)
Cl(2)	0.52363 (14)	0.22871 (13)	0.40200 (11)
O(2A)	0.4671 (7)	0.2995 (5)	0.4185 (6)
O(2B)	0.4651 (6)	0.1643 (5)	0.3695 (9)
O(2C)	0.5646 (7)	0.1994 (8)	0.4737 (5)
O(2D)	0.5774 (7)	0.2427 (11)	0.3404 (6)
Cl(3)[b]	0.02896 (13)	0.26864 (12)	0.08349 (11)
O(3A)	0.0704 (7)	0.2959 (6)	0.0111 (5)
O(3B)	−0.0233 (9)	0.3330 (6)	0.1189 (9)
O(3C)	−0.0547 (9)	0.2347 (18)	0.0508 (10)
O(3D)	0.0914 (12)	0.2946 (13)	0.1483 (9)
O(3E)	−0.0023 (16)	0.1906 (9)	0.0932 (14)
O(3F)	0.0780 (15)	0.2062 (19)	0.1183 (19)
C(1)	0.2118 (6)	0.4717 (5)	0.0872 (5)
Cl(4)	0.13958 (16)	0.54942 (13)	0.03951 (13)
Cl(5)	0.31942 (15)	0.46696 (16)	0.03545 (14)
Cl(6)	0.23228 (15)	0.49234 (13)	0.19761 (11)

[a] Atoms are labeled as shown in Figure 1. Primed values refer to the alternate positions of the disordered perchlorate groups. Estimated standard deviations in the last significant digits are given in parentheses. [b] Disordered perchlorate group.

Scattering factors for the hydrogen atoms were those of Stewart et al.[13] All hydrogen atoms except the one on the bridging hydroxide were placed in calculated positions (C–H = 0.95 Å, N–H = 0.87 Å). The methylene hydrogen atoms were permitted to ride on the carbon atoms to which they were attached and constrained to an ideal geometry. The positions of the amine and chloroform hydrogen atoms were not refined. All hydrogen atoms were given a group temperature factor that was allowed to refine.

The function minimized during the least-squares refinement was $\sum w(|F_o| - |F_c|)^2$ where $w = \kappa/[\sigma^2(F_o) + 0.0004(F_o)^2]$, where κ refined to 1.49. The discrepancy indices[14] converged at 0.058 and 0.075, respectively, for 452 parameters and 4305 reflections with $F \geq 4\sigma(F)$. In the final cycles of refinement some parameters associated with the disordered bridging perchlorate shifted by $\pm 1\sigma$. No other variable shifted more than 0.2 of its esd. The largest peak on the final difference Fourier map, ~1 eÅ^{-3}, was equidistant from the three chlorine atoms of the chloroform and about 1 Å from the carbon atom, on the opposite side from the hydrogen. The remaining peaks were all less than 0.85 eÅ^{-3}. The average $w\Delta^2$ for groups of data sectioned according to parity group, $|F_o|$, sin θ/λ, and $|h|,|k|,|l|$, showed reasonable consistency, and the weighting scheme was considered to be satisfactory.

(13) Stewart, R. F.; Davidson, E. R.; Simpson, W. T. *J. Chem. Phys.* **1965**, *42*, 3175.

(14) $R_1 = \sum||F_o| - |F_c||/\sum|F_o|$; $R_2 = [\sum w(|F_o| - |F_c|)^2/\sum w|F_o|^2]^{1/2}$.

Table III. Final Positional Parameters for $[Cu_2(OAc)_2A](ClO_4)_2$ (2)[a]

atom	x	y	z
Cu	0.26838 (14)	0.10289 (10)	0.51169 (7)
Cl	0.8181 (3)	0.4216 (3)	0.66052 (16)
O(11)	0.0155 (11)	0.5697 (9)	0.3165 (5)
O(12)	0.2469 (11)	0.6630 (8)	0.2909 (6)
O(13)	0.2501 (11)	0.4555 (8)	0.3364 (6)
O(14)	0.2129 (13)	0.6262 (10)	0.4152 (6)
O(1)	0.2801 (7)	−0.0747 (5)	0.5467 (4)
O(2)	0.4549 (7)	0.0930 (7)	0.4323 (4)
C(11)	0.5904 (11)	0.1358 (9)	0.4325 (5)
C(12)	0.6081 (13)	0.2698 (10)	0.4011 (8)
N(1)	0.4191 (9)	0.1881 (8)	0.6007 (5)
C(1)	0.3969 (13)	0.3282 (10)	0.5951 (7)
C(2)	0.2397 (16)	0.3589 (10)	0.5528 (7)
N(2)	0.2006 (12)	0.2844 (8)	0.4852 (6)
C(3)	0.0403 (11)	0.2846 (9)	0.4414 (6)
C(4)	0.0437 (13)	0.1838 (9)	0.3806 (6)
N(3)	0.0906 (8)	0.0603 (7)	0.4227 (4)
C(5)	−0.1332 (12)	0.0444 (9)	0.6312 (6)
C(6)	0.0006 (11)	0.0771 (10)	0.6924 (6)
O	0.1393 (7)	0.1031 (7)	0.6574 (3)
C(7)	0.2691 (12)	0.1534 (11)	0.7089 (6)
C(8)	0.4245 (11)	0.1342 (10)	0.6793 (5)

[a] Atoms are labeled as shown in Figure 2. Estimated standard deviations, given in parentheses, occur in the last significant digits.

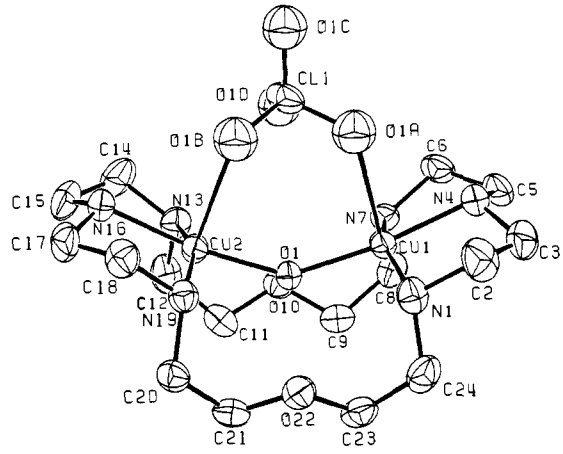

Figure 1. Molecular structure of the $[Cu_2(OH)(ClO_4)\subset A]^{2+}$ cation showing the 40% thermal ellipsoids. For clarity the diagram depicts only one of two possible positions of the model for the disordered perchlorate. The oxygen atoms of the perchlorate were arbitrarily assigned as spheres of 0.3-Å radius. Hydrogen atoms are omitted.

Compound 2. The structure was solved by Patterson and Fourier methods and refined as described above for compound **1**.[11] The hydrogen atoms of the methyl group were allowed to refine as a rigid rotor. The function minimized during the least-squares refinement was $\sum w(|F_o| - |F_c|)^2$ where $w = \kappa/[\sigma^2(F_o) + 0.0004(F_o)^2]$; κ refined to 1.800. The discrepancy indices[14] converged at $R_1 = 0.087$ and $R_2 = 0.095$. During the final cycle of least-squares refinement, the rotation of the methyl group about the C–C bond changed by 1σ, the next largest change in a parameter was 0.2σ, and most parameters changed by less than 0.1σ. The final difference maps showed four peaks close to the copper atom greater than 1 eÅ^{-3}. The largest was ~2 eÅ^{-3}. The absorption correction reduced the intensity of these peaks but did not completely eliminate them. The average $w\Delta^2$ for groups of data sectioned as previously described showed reasonable consistency, and the weighting scheme was considered to be acceptable.

Results and Discussion

Description and the Structures. The final non-hydrogen atomic positional and thermal parameters with standard deviations appear in Tables II and III. Interatomic distances and angles are reported

Table IV. Interatomic Distances (Å) and Angles (deg) for $[Cu_2(OH)(ClO_4)\subset A](ClO_4)_2 \cdot CHCl_3$ (1)[a]

Coordination Sphere			
Cu(1)-O(1)	1.922 (4)	Cu(2)-O(1)	1.912 (4)
Cu(1)-N(1)	2.054 (5)	Cu(2)-N(13)	2.057 (5)
Cu(2)-N(4)	1.995 (5)	Cu(2)-N(16)	1.993 (5)
Cu(1)-N(7)	2.041 (5)	Cu(2)-N(19)	2.056 (5)
Cu(1)-O(1A)	2.540 (8)	Cu(2)-O(1B)	2.568 (8)
Cu(1)-Cu(2)	3.642	Cu(1)-O(1)-Cu(2)	143.6 (2)
O(1)-Cu(1)-N(1)	95.6 (2)	O(1)-Cu(2)-N(13)	96.0 (2)
O(1)-Cu(1)-N(4)	171.9 (2)	O(1)-Cu(2)-N(16)	170.6 (2)
O(1)-Cu(1)-N(7)	96.7 (2)	O(1)-Cu(2)-N(19)	96.0 (2)
O(1)-Cu(1)-O(1A)	91.7 (3)	O(1)-Cu(2)-O(1B)	90.6 (2)
N(1)-Cu(1)-N(4)	85.7 (2)	N(13)-Cu(2)-N(16)	85.3 (2)
N(1)-Cu(1)-N(7)	158.3 (2)	N(13)-Cu(2)-N(19)	160.5 (2)
N(1)-Cu(1)-O(1A)	108.3 (3)	N(13)-Cu(2)-O(1B)	109.5 (3)
N(4)-Cu(1)-N(7)	84.6 (2)	N(16)-Cu(2)-N(19)	85.3 (2)
N(4)-Cu(1)-O(1A)	80.3 (3)	N(16)-Cu(2)-O(1B)	80.2 (3)
N(7)-Cu(1)-O(1A)	89.1 (3)	N(19)-Cu(2)-O(1B)	85.7 (3)
Ligand Geometry			
N(1)-C(2)	1.481 (9)	C(12)-N(13)	1.474 (9)
N(1)-C(24)	1.497 (9)	N(13)-C(14)	1.473 (9)
C(2)-C(3)	1.509 (11)	C(14)-C(15)	1.479 (10)
C(3)-N(4)	1.479 (9)	C(15)-N(16)	1.475 (9)
N(4)-C(5)	1.466 (8)	N(16)-C(17)	1.469 (8)
C(5)-C(6)	1.513 (10)	C(17)-C(18)	1.502 (10)
C(6)-N(7)	1.471 (8)	C(18)-N(19)	1.480 (8)
N(7)-C(8)	1.483 (8)	N(19)-C(20)	1.489 (8)
C(8)-C(9)	1.507 (9)	C(20)-C(21)	1.488 (9)
C(9)-O(10)	1.413 (8)	C(21)-O(22)	1.420 (8)
O(10)-C(11)	1.435 (8)	O(22)-C(23)	1.433 (8)
C(11)-C(12)	1.505 (10)	C(23)-C(24)	1.484 (10)
Cu(1)-N(1)-C(2)	105.5 (4)	Cu(2)-N(13)-C(12)	120.4 (4)
Cu(1)-N(1)-C(24)	118.1 (4)	Cu(2)-N(13)-C(14)	104.8 (4)
C(2)-N(1)-C(24)	110.7 (5)	C(12)-N(13)-C(14)	110.5 (5)
N(1)-C(2)-C(3)	110.3 (6)	N(13)-C(14)-C(15)	110.3 (6)
C(2)-C(3)-N(4)	106.4 (6)	C(14)-C(15)-N(16)	106.4 (6)
Cu(1)-N(4)-C(3)	108.5 (4)	Cu(2)-N(16)-C(15)	107.9 (4)
Cu(1)-N(4)-C(5)	109.9 (4)	Cu(2)-N(16)-C(17)	109.0 (4)
C(3)-N(4)-C(5)	116.9 (5)	C(15)-N(16)-C(17)	119.2 (5)
N(4)-C(5)-C(6)	106.5 (5)	N(16)-C(17)-C(18)	107.6 (5)
C(5)-C(6)-N(7)	108.9 (5)	C(17)-C(18)-N(19)	109.5 (5)
Cu(1)-N(7)-C(6)	106.8 (4)	Cu(2)-N(19)-C(18)	105.8 (4)
Cu(1)-N(7)-C(8)	116.3 (4)	Cu(2)-N(19)-C(20)	118.7 (4)
C(6)-N(7)-C(8)	111.0 (5)	C(18)-N(19)-C(20)	111.1 (5)
N(7)-C(8)-C(9)	112.4 (5)	N(19)-C(20)-C(21)	112.1 (5)
C(8)-C(9)-O(10)	107.4 (5)	C(20)-C(21)-O(22)	107.9 (5)
C(9)-O(10)-C(11)	114.8 (5)	C(21)-O(22)-C(23)	115.7 (5)
O(10)-C(11)-C(12)	107.2 (5)	O(22)-C(23)-C(24)	108.6 (5)
C(11)-C(12)-N(13)	112.9 (5)	C(23)-C(24)-N(1)	112.9 (5)
Chloroform Geometry			
C(1)-Cl(4)	1.734 (8)	Cl(4)-C(1)-Cl(5)	111.1 (4)
C(1)-Cl(5)	1.779 (8)	Cl(4)-C(1)-Cl(6)	112.1 (4)
C(1)-Cl(6)	1.764 (8)	Cl(5)-C(1)-Cl(6)	109.0 (4)

Perchlorate Geometry

	Cl-O			O-Cl-O		
group	min	max	mean[b]	min	max	mean[b]
perchlorate 1	1.30 (2)	1.38 (2)	1.32 (4)	90 (2)	124 (2)	109.3 (12.7)
perchlorate 1'	1.27 (2)	1.42 (2)	1.34 (6)	77 (2)	121 (2)	108.3 (19.2)
perchlorate 2	1.27 (2)	1.39 (1)	1.35 (5)	103.1 (8)	115.0 (7)	109.2 (4.5)
perchlorate 3[c]	1.29 (2)	1.40 (2)	1.35 (5)	53 (2)	155 (1)	101 (28)

Possible Hydrogen Bonding Interactions			
O(1)-O(10)	3.021 (6)	O(1)-O(22)	2.965 (6)
Cu(1)-O(1)-O(10)	95.57 (16)	Cu(1)-O(1)-O(22)	98.57 (16)
Cu(2)-O(1)-O(10)	97.95 (16)	Cu(2)-O(1)-O(22)	97.94 (16)

[a] See footnote *a*, Table II. Distances have not been corrected for thermal motion. [b] $\sigma(\text{mean}) = [(\Sigma x_i^2 - \bar{n}\bar{x}^2)/(n-1)]^{1/2}$. [c] Badly disordered group.

Table V. Interatomic Distances (Å) and Angles (deg) for $[Cu_2(OAc)_2A]_n(ClO_4)_{2n}$ (2)[a]

Copper Coordination Geometry			
Cu-N(1)	2.063 (8)	Cu-O(1)	1.948 (6)
Cu-N(2)	2.009 (9)	Cu-O(2)	2.277 (7)
Cu-N(3)	2.047 (7)		
N(1)-Cu-N(2)	83.8 (3)	N(2)-Cu-O(1)	82.9 (3)
N(1)-Cu-N(3)	166.0 (3)	N(2)-Cu-O(2)	95.8 (4)
N(1)-Cu-O(1)	100.0 (3)	N(3)-Cu-O(1)	91.8 (3)
N(1)-Cu-O(2)	94.5 (3)	N(3)-Cu-O(2)	91.1 (3)
N(2)-Cu-N(3)	82.9 (3)	O(1)-Cu-O(2)	98.4 (3)
Acetate Geometry			
C(11)-O(1)	1.27 (11)	Cu-O(2)-C(11)	136.2 (6)
C(11)-O(2)	1.234 (12)	O(1)-C(11)-O(2)	125.7 (9)
C(11)-C(12)	1.517 (15)	O(1)-C(11)-C(12)	115.7 (8)
Cu-O(1)-C(11)	124.3 (6)	O(2)-C(11)-C(12)	118.6 (8)
Ligand Geometry			
N(1)-C(1)	1.437 (13)	C(4)-N(3)	1.507 (12)
N(1)-C(8)	1.491 (13)	N(3)-C(5)	1.528 (13)
C(1)-C(2)	1.457 (16)	C(5)-C(6)	1.478 (13)
C(2)-N(2)	1.417 (15)	C(6)-O	1.440 (12)
N(2)-C(3)	1.455 (13)	O-C(7)	1.412 (12)
C(3)-C(4)	1.504 (14)	C(7)-C(8')	1.507 (15)
Cu-N(1)-C(1)	108.5 (6)	C(3)-C(4)-N(3)	106.1 (8)
Cu-N(1)-C(8)	118.0 (6)	Cu-N(3)-C(4)	107.4 (5)
C(1)-N(1)-C(8)	114.9 (8)	Cu-N(3)-C(5)	114.4 (5)
N(1)-C(1)-C(2)	110.4 (8)	C(4)-N(3)-C(5)	111.9 (7)
C(1)-C(2)-N(2)	112.6 (10)	N(3)-C(5)-C(6)	112.9 (8)
Cu-N(2)-C(2)	107.4 (7)	C(5)-C(6)-O	108.5 (8)
Cu-N(2)-C(3)	109.5 (6)	C(6)-O-C(7)	113.8 (7)
C(2)-N(2)-C(3)	121.4 (10)	O-C(7)-C(8')	111.5 (8)
N(2)-C(3)-C(4)	104.8 (8)	C(7')-C(8)-N(1)	111.9 (7)
Perchlorate Geometry			
Cl-O(11)	1.410 (9)	O(11)-Cl-O(13)	109.3 (5)
Cl-O(12)	1.402 (10)	O(11)-Cl-O(14)	108.9 (6)
Cl-O(14)	1.409 (9)	O(12)-Cl-O(13)	110.1 (6)
Cl-O(14)	1.411 (10)	O(12)-Cl-O(14)	108.9 (6)
O(11)-Cl-O(12)	109.8 (5)	O(13)-Cl-O(14)	109.9 (6)

[a] See footnote *a*, Table III. Distances have not been corrected for thermal motion.

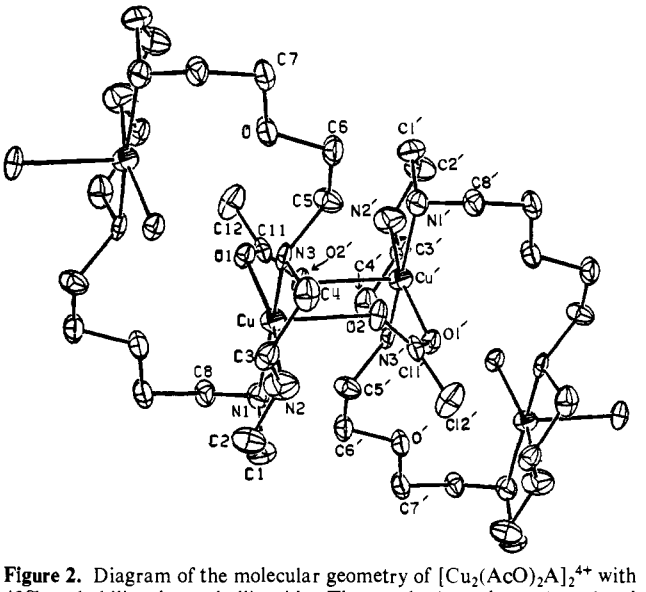

Figure 2. Diagram of the molecular geometry of $[Cu_2(AcO)_2A]_2^{4+}$ with 40% probability thermal ellipsoids. The numbering scheme (unprimed set) of the crystallographically unique atoms is shown. The polymer chain is propagated by inversion centers, and symmetry-related atoms are primed.

in Tables IV and V. A listing of hydrogen atom positions, thermal parameters for all atoms, and observed and calculated structure factors is available as supplementary material (Tables S1–S6). Figure 1 shows the molecular struture of the $[Cu_2(OH)(ClO_4)\subset A]^{2+}$ cation, while Figure 2 depicts the geometry of two $[Cu_2(OAc)_2A]^{2+}$ units.

$[Cu_2(OH)(ClO_4)\subset A](ClO_4)_2 \cdot CHCl_3$ (1). The structure consists of a discrete $[Cu_2(OH)(ClO_4)\subset A]^{2+}$ ion, two perchlorate anions, and one chloroform molecule in the asymmetric unit. An approximate twofold axis passes through the oxygen atom of the bridging hydroxide ion, which relates the two independent copper atoms to each other (Figure 1). This pseudosymmetry leads to the two independent copper atoms having very similar coordination geometries. The geometry around the copper atoms is distorted square pyramidal. Three of the basal plane positions are taken up by the amine nitrogen atoms of the diethylenetriamine unit of the macrocycle. The other basal site contains the single hydroxide ion that bridges both copper atoms.

The Cu–O bond lengths compare favorably with distances in other mono-[7] and dihydroxo-bridged[15] copper complexes. The Cu–O–Cu angle, 143.6 (2)°, is larger than that seen in the dihydroxo-bridged complexes but comparable to that in the monohydroxo-bridged complexes. The Cu–N bond lengths and N–Cu–N angles are typical of square-planar diethylenetriamine complexes.[16]

Until recently, not many structures of the monohydroxo-bridged dicopper(II) ion had been reported, whereas dihydroxo-bridged dicopper(II) complexes have been well studied. Because of the steric restrictions of having two one-atom bridges, the Cu–O–Cu angles found in the dihydroxo-bridged complexes are more acute (95–104°)[15] than the one found in the present complex. Monohydroxo-bridged dichromium complexes exhibit a range of M–O–M angles (135.4–165.6°)[17] that embraces the angle 143.6 (2)° found in the present macrocyclic complex. Most of the known monohydroxo-bridged dicopper(II) complexes[7a,c,d] have similar M–O–M angles, as do monoalkoxy-bridged dicopper(II) compounds.[18] An exception is $[Cu_2(OH)(OH_2)L^2](ClO_4)_3 \cdot 2H_2O$,[7e] which has Cu–OH–Cu = 110.3 (7)°, but this compound is claimed also to have a Cu–OH_2–Cu bridge; L^2 is a Schiff base binucleating macrocycle.

A disordered perchlorate anion also bridges the two copper atoms (Figure 1) through long axial bonds (2.55 Å av). The bridging occurs in a manner similar to that found previously in $[Cu(DMAEP)(OH)(ClO_4)]_2$, where DMAEP = 2-[2-(dimethylamino)ethyl]pyridine,[19] but different from the structural mode found in perchlorate-bridged copper(II) polymers.[20] The disordered perchlorate is a composite of two overlapping, half-occupancy perchlorate groups related to each other by the pseudotwofold axis that also relates the two copper atoms. On the first difference Fourier map the perchlorate group had the appearance of a chlorine atom ringed by three coplanar oxygen atoms. Two half-occupancy oxygen atoms were found with long Cl–O bond lengths approximately normal to the plane of the other oxygen atoms. When the thermal parameters of the chlorine and the three full-occupancy oxygen atoms were allowed to refine anisotropically, the thermal ellipsoids of these four atoms were greatly elongated normal to their mean plane. This result indicated that these atoms were two overlapping, half-occupancy ClO_4^- groups. From the two axial Cl–O bond lengths it was calculated that the two disordered chlorine atoms should be about 0.45 Å apart. Two half-occupancy chlorine atoms placed 0.45 Å apart eventually refined to a distance 0.49 (2) Å apart. The replacement of the oxygen atoms with two interlocking rigid-body perchlorate groups with isotropic group thermal parameters refined and made chemical sense. The final mode of the perchlorate group included the two half-occupancy chlorine atoms Cl(1) and Cl(1′), three full-occupancy oxygen atoms O(1A), O(1B), O(1C), and two half-occupancy oxygen atoms O(1D) and O(1D′). Further details are given in ref 8.

There is another disordered perchlorate anion in the structure. It was refined in a similar manner, but this group was not well-behaved. Although the final model employed accounted for the electron density, the resulting geometry (Table IV) is meaningless. The third perchlorate, by contrast, was well-behaved, as was the chloroform molecule. The geometry of both is acceptable.

The hydrogen atom of the bridging hydroxide ion was not found, even upon very careful examination of difference Fourier maps. Residual electron density caused by proximity to the disordered bridging perchlorate group may have contributed to the difficulty in locating the hydroxyl proton. Because there are few high quality monohydroxo-bridged dicopper(II) structures, it is not clear whether to expect the proton to be displaced from the Cu–O–Cu plane. In $[(bpy)_2Cu{-}OH{-}Cu(bpy)_2](ClO_4)_3$[7a] it appears that the hydrogen atom of the bridging hydroxide lies in the Cu–O–Cu plane since the sum of the three angles around the oxygen atom is 360.0°. A similar result holds for the series of Cr–OH–Cr structures.[17] In one Cr–OH–Cr structure, however, the hydrogen atom of the bridging hydroxide ion was found to be 0.48 Å out of the Cr–O–Cr plane.[17b] The variability in the position of the hydrogen atom in these examples makes it impossible to calculate its position for **1**. If it were ordered it should have shown up on the difference map. It is therefore more likely that the hydrogen atom in **1** is disordered over two positions, in a plane equidistant from the copper atom, where it is hydrogen bonded to the ether oxygen atoms of the macrocycle. As can be seen in Figure 1, these ether oxygens are positioned well to accept such a hydrogen bond. Displacement of the hydrogen atom from the Cu–O–Cu plane could have magnetic significance.

The infrared spectrum shows absorbances in the O–H, N–H stretching frequency region at 3472, 3288, and 3264 cm^{-1}. The absorbance at 3472 cm^{-1} is in the correct energy region for O–H stretches, as revealed by studies of other known monohydroxo-bridged dicopper(II) complexes.[7a,b,e] Its precise value is no doubt affected by the proposed hydrogen bonding. The deuteration experiment distinguished the N–D from the O–D stretches. Upon deuteration the frequency of the N–H stretches shifted more than that of the O–H stretch, as expected; making the usual assumptions,[21] both the O–D and N–D stretches shifted by 96% of the theoretical value. There is thus no doubt that compound **1** contains a bridging hydroxo and not an oxo group, even though the exact position of the hydrogen atom is unknown. Selected angles and distances for possible hydrogen bonding of the hydroxide with the two ether oxygen atoms of the macrocycle are given in Table IV.

The internal geometry of the macrocycle is normal. As may be seen from Figure 1, the macrocycle is considerably less extended in compound **1**, where the Cu–Cu distance is 3.64 Å, than in $[Cu_2(im)\subset A]^{3+}$, in which the Cu–Cu distance is 5.87 Å.[2c] It seems that the macrocycle, while limiting the maximum distance that the two copper atoms may be separated from each other, does not severely restrict the minimum distance. In this respect macrocycle A is similar to the crown ethers, which fold up around ions that are too small for the cavity, as in NaSCN 18-crown-6.[22a] Alternatively, they may act as an equatorial girth for an ion of the correct size, as in KSCN 18-crown-6,[22b] or sit on the side of an ion too large for the cavity, as in CsSCN 18-crown-6.[22c] Further discussion of the folding and torsion angles of A in compound **1** and related complexes is given below.

Examination of the crystal packing diagram[8] shows that the perchlorate ions are situated in channels that run parallel to the *c* axis. The channels on the edges of the unit cell contain the disordered perchlorate, while the ones in the interior of the cell are ordered. There are no strong hydrogen bonds to the per-

(15) Hodgson, D. J. *Prog. Inorg. Chem.* **1975**, *19*, 173.
(16) O'Young, C.-L.; Dewan, J. C.; Lilienthal, H. R.; Lippard, S. J. *J. Am. Chem. Soc.* **1978**, *100*, 7271 and references cited therein.
(17) (a) Cline, S. J.; Glerup, J.; Hodgson, D. J.; Jensen, G. S.; Pedersen, E. *Inorg. Chem.* **1981**, *20*, 2229. (b) Hodgson, D. J.; Pedersen, E. *Ibid.* **1980**, *19*, 3116. (c) Kaas, K. *Acta Crystallogr., Sect. B* **1979**, *B35*, 1603.
(18) McKee, V.; Dagdigian, J. V.; Bau, R.; Reed, C. A. *J. Am. Chem. Soc.* **1981**, *103*, 7000.
(19) Lewis, D. L.; Hatfield, W. E.; Hodgson, D. J. *Inorg. Chem.* **1974**, *13*, 147.
(20) (a) Ray, N.; Tyagi, S.; Hathaway, B. *Acta Crystallogr., Sect. B* **1982**, *B38*, 1574. (b) See also the discussion in: Belin, C. H.; Chaabouni, M.; Pascal, J. L.; Potier, J. *Inorg. Chem.* **1982**, *21*, 3577.
(21) Shoemaker, D. P.; Garland, C. W. "Experiments in Physical Chemistry"; McGraw-Hill: New York, 1962.
(22) (a) Dobler, M.; Dunitz, J. D.; Seiler, P. *Acta Crystallogr., Sect. B* **1974**, *B30*, 2741. (b) Seiler, P.; Dobler, M.; Dunitz, J. D. *Ibid.* **1974**, *B30*, 2744. (c) Dobler, M.; Phizackerley, R. P. *Ibid.* **1974**, *B30*, 2748.

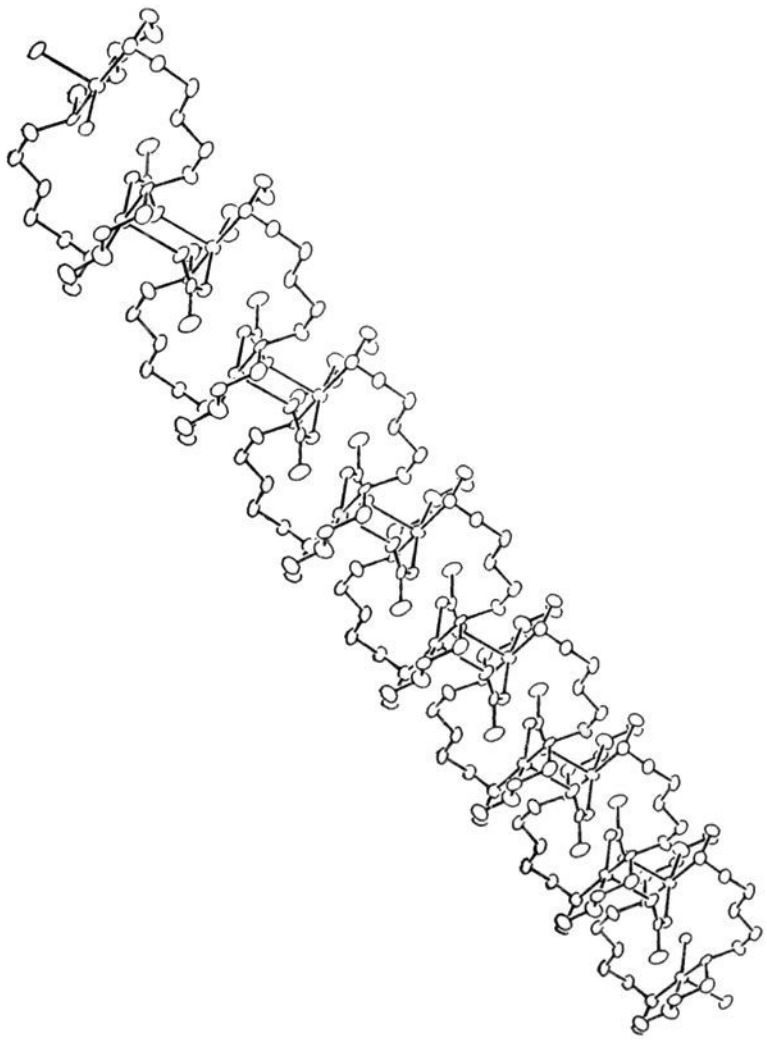

Figure 3. Diagram of $[Cu_2(AcO)_2A]_n^{2n++}$ where $n = 7$, showing the polymer chain propagated along the *a* direction.

chlorate group that would order them. The closest contact between one of the oxygen atoms on the ordered perchlorate and another atom is 3.10 (1) Å to N1.

From a crystallographic point of view, one interesting aspect of this structure is the pseudosymmetry in the cell. A pseudo-twofold axis relates not only the two copper atoms but both halves of almost the entire structure. An atom at (x,y,z) is related to another at $(^1/_2 - x,-y,z)$. This condition corresponds to a twofold axis parallel to z passing through $x = {}^1/_4$ and $y = 0$. The deviation of the pairs of atoms from this twofold relationship is given in ref 8. If β were 90° and the twofold symmetry axis were a real one, simple considerations[8] show the result to be the orthorhombic space group *Pnca*, a nonstandard setting of *Pbcn* (D_{2h}^{14}, No. 60).[10] The chloroform molecule keeps the structure from adopting the more symmetric orthorhombic space group. In *Pbcn* it would have to occupy a position of twofold symmetry. The fact that chloroform does not contain twofold symmetry seems to be what requires the monoclinic cell. If carbon tetrachloride or methylene chloride had been diffused into the solution instead of chloroform, the crystals might well have crystallized in *Pbcn*.

$[Cu_2(OAc)_2A]_n(ClO_4)_{2n}$ (2). The strucure consists of a linear polymer of $[Cu_2(OAc)_2A]_n^{2n}$ cations, propagated along the *a* crystallographic axis (Figure 3), and ClO_4^- counterions. Individual macrocycles are connected by di(μ-acetato)dicopper(II) bridged units, the two halves of which are related by an inversion center (Figure 4). The coordination geometry around the copper atoms is square pyramidal. Three of the basal coordination sites are occupied by the nitrogen atoms of the diethylenetriamine portion of the macrocycle. The bond lengths from the copper atom to these three nitrogen atoms are normal (Table IV), with the shortest bond being to the central nitrogen atom, as usual.[16] To the fourth basal site is coordinated an oxygen atom of the bridging acetate group. The Cu–O bond length, 1.948 (6) Å, is also the expected value.[23] Through a longer bond, 2.278 (6) Å, to an axial site of the copper atom is coordinated an oxygen atom of an inversion-related acetate group. The copper is displaced 0.18 Å from the mean plane of the four basal ligands toward the axial ligand.

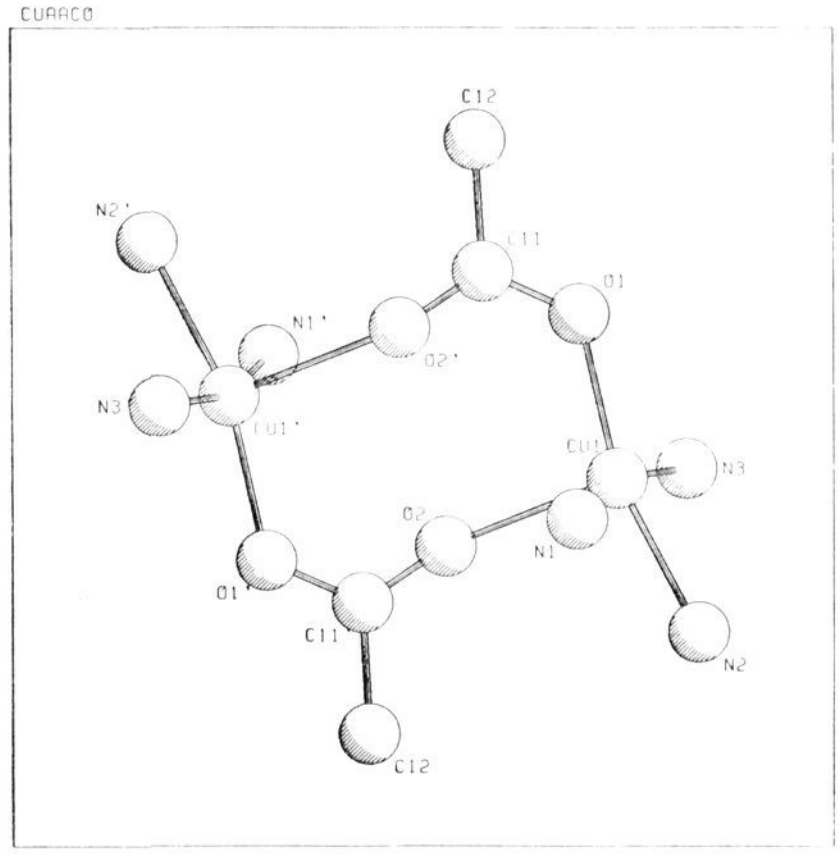

Figure 4. Diagram of the copper coordination geometry in $[Cu_2(AcO)_2A]_n^{2n+}$. The copper center is square pyramidal with N1, N2, N3, and O1 in the basal plane. Atoms N1, N2, and N3 are related to N1′, N2′, and N3′ by an inversion center but are in adjacent macrocycles. The acetate bridge has a syn–anti configuration.

The copper atoms in the same macrocycle are bridged only by the two bis(2-aminoethyl) ether chains. Thus instead of the $[Cu_2(OAc)]^{3+}$ unit being incorporated, like imidazolate,[2] into the binucleating macrocycle A, a bridged binuclear $[Cu_2(OAc)_2]^{2+}$ complex links different macrocycles in a polymeric structure.

The two acetate groups bridge from the basal position of one copper atom to an axial position of the other by adopting a syn–anti conformation, as can easily be seen in Figure 4. Acetate is capable of bridging metal atoms in a variety of modes. In $[Cu(AcO)_2(H_2O)]_2$, the acetate groups bridge the copper atoms in a syn–syn mode, which leads to a short Cu–Cu distance.[24] There are a variety of related structures with aliphatic and aromatic carboxy cyclic acids in place of the acetate.[25] Oxydiaceate bridges two copper atoms in a syn–anti configuration,[26] but in contrast to **2**, both bonds to the copper atoms are strong. Formate[27] and carbonate,[28] in related structures, also bridge copper atoms in a syn–anti configuration. The influence of these stereochemical differences on the magnetic properties of these compounds is discussed below.

The internal geometry of ligand A is normal. The conformation of the macrocycle in compound **2**, however, is very different from that in $[Cu_2(im)(imH)_2{\subset}A](ClO_4)_3$ and $[Cu_2(OH)(ClO_4){\subset}A](ClO_4)_2{\cdot}CHCl_3$ (**1**). As illustrated in Figure 5, the macrocycle in $[Cu_2(im)(imH)_2{\subset}A]^{3+}$ is stretched and reasonably planar to enclose the Cu–im–Cu^{3+} ion; in **1** it is folded up in a U shape to accommodate the Cu–OH–Cu^{3+} ion; the macrocycle in **2** is in an S conformation. Some insight into these conformational differences is provided by examining the torsion angles of the macrocycle, which are listed in Table S7. To identify these torsion angles we use the atom-labeling scheme of the hydroxo-bridged complex (Figure 5) and the sign convention of ref 29.

The allowed conformations of an aliphatic 24-membered ring with no substituents are numerous. Complexation of two copper

(23) Lingafelter, E. C.; Braun, R. L. *J. Am. Chem. Soc.* **1968**, *88*, 2951.

(24) van Niekirk, J. N.; Scholning, F. K. L. *Acta Crystallogr.* **1953**, *6*, 227.

(25) (a) Lewis, J.; Mabbs, F. E.; Royston, L. K.; Smail, W. R. *J. Chem. Soc. A* **1969**, 291. (b) Martin, R. L.; Watermann, R. *J. Chem. Soc.* **1957**, *2545*.

(26) Whitlow, S. H.; Davey, G. *J. Chem. Soc. Dalton Trans.* **1975**, 1228.

(27) Barclay, G. A.; Kennard, C. H. L. *J. Chem. Soc.* **1961**, 3289.

(28) Kolks, G.; Lippard, S. J.; Waszczak, J. V. *J. Am. Chem. Soc.* **1980**, *102*, 4832 and references cited therein.

(29) Allen, F. H.; Rogers, O. *Acta Crystallogr.*, Sect. *B* **1969**, *B25*, 1326.

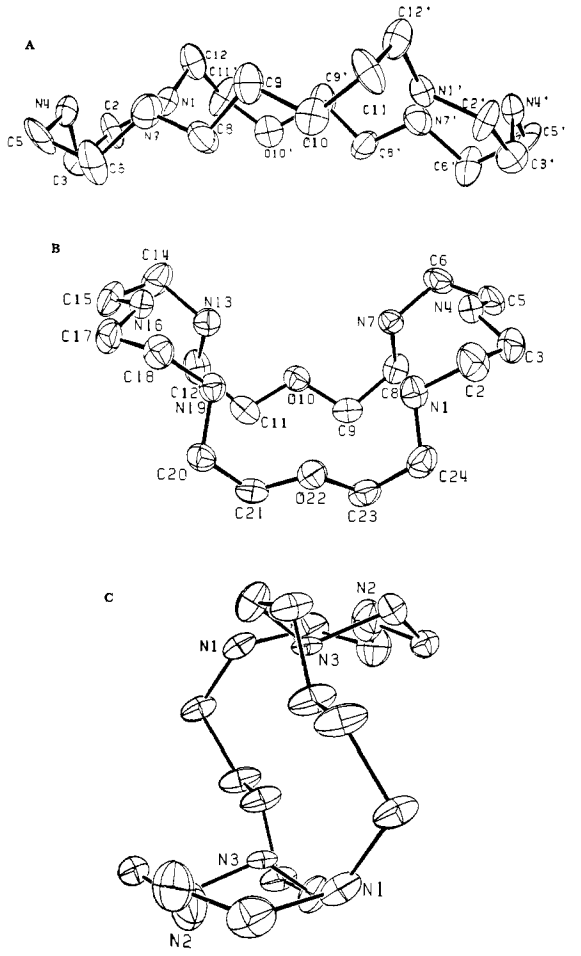

Figure 5. Diagram of (A) the planar conformation of macrocycle A in the complex $[Cu_2(im)(imH)_2 \subset A](ClO_4)_3$. (B) U-shaped conformation of macrocycle A in the complex $[Cu_2(OH)(ClO_4) \subset A](ClO_4)_2 \cdot CHCl_3$. (C) S-shaped conformation of macrocycle A in the complex $[Cu_2(OAc)_2A]_n(ClO_4)_{2n}$.

atoms reduces the largest ring size to 16 members and constrains the allowed conformations. The major congruencies in structure are expected to occur in the diethylenetriamine portions of the macrocycle. Examination of torsion angles about the periphery of the macrocycle, particularly in the (C,N,C,C) type 1[30] dihedral angles, reveals few consistent trends. When the (Cu,N,C,C,) dihedral angles are included, however, a pattern begins to emerge. All the torsion angles around the diethylenetriamine portion of the macrocycle are acute. They are $\sim \pm 60°$ for the (N,C,C,N) angles and $\pm 40°$ for the (Cu,N,C,C) angles. The torsion angles of the hydroxo- and acetate-bridged complexes follow the same alternating sign sequence around the diethylenetriamine portion of the ring. The imidazolate-bridged compound exhibits a similar pattern except at N(4), where both the [Cu–N(4)–C(3)–C(2)] and [Cu–N(4)–C(5)–C(6)] angles have the same sign. These two patterns correspond to two different foldings of the five-membeed ethylenediamine–copper chelate rings. With reference to the N(1)–Cu(1)–N(4) and N(4)–Cu(1)–N(7) planes, the hydroxo- and acetate-bridged complexes are in a C(3)-exo, C(5)-exo conformation,[30] whereas the imidazolate-bridged complex has C-(3)-exo, C(5)-endo. The difference in conformation at N(4) corresponds to a rotation about the Cu–N(4) bond. The other

(30) Nomenclature: For torsional angle A(I,J,K,L), dihedral angle type 1 is defined as that between the JI vector and KL vector when projected onto the plane with normal KJ. The sign is positive when JI is rotated clockwise into KL and negative for counterclockwise rotation. Type 2 and 3 dihedral angles are similar to type 1 except that both I and L are bonded to the same atom, J or K for types 2 and 3, respectively;[29] endo and exo mean the same and opposite sides, respectively, of the N–Cu–N plane, with the reference side being the side with axial coordination.

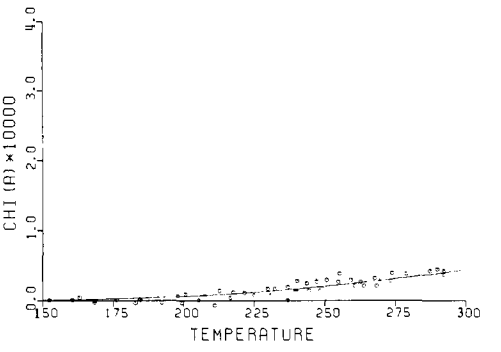

Figure 6. Plot of the corrected atomic (per copper ion) susceptibility of **1** as a function of temperature. The susceptibility is in cgs units and the temperature is in K. The open circles are the experimental data from two independent determinations. The solid line is the result of the least-squares fitting of the coupling constant, J, in the Bleaney–Bowers equation to the experimental data (see text).

torsion angles do not follow as consistent a pattern. The break occurs at the torsion angles just at the end of the diethylenetriamine unit, such as A[C(2),N(1),C(24),C(23)] and A[Cu, N(1),C(24),C(23)]. Even a high-energy conformation where both of these angles are acute, A[Cu,N(1),C(8),C(7)], −66°, and A[C(1),N(1),C(8),C(7′)], +64°, occurs in the acetate-bridged polymer. In all other instances one of the angles is approximately linear. As expected, torsion angles around the ether oxygen atoms are linear, with the single exception of one angle in the imidazolate-bridged complex, where A[C(9),O(10),C(11),C(12′)] is −80°.

Considering only the torsion angles of the macrocycle, that is, ignoring the torsion angles involving the copper atoms, there are some general trends. In the two complexes that enclose the bridged dicopper ions, half the torsion angles are linear and the other half are equally distributed between positive and negative values. This equal distribution of positive and negative angles is required for the macrocycle to assume a conformation necessary for encircling a bridged dicopper ion. In the acetate-bridged polymer, the macrocycle has an excess of negative torsion angles (ratio of 2:5:5 for positive:negative:linear), which causes the S conformation.

Examination of CPK space-filling models reveals many additional allowed conformations with copper bound to the diethylenetriamine poles of the macrocycle that have not yet been seen. It should be possible, for example, to have the syn–anti monoacetate-bridged dicopper(II) ion enclosed by the macrocycle. Many of the other conformations involve close axial–axial and axial–equatorial intermetallic interactions which will be important with metal ions other than copper(II).

The perchlorate anion in compound **2** is well-behaved. The Cl–O bond lengths are 1.40 (1), 1.41 (1), 1.44 (1), and 1.46 (1) Å when corrected for thermal motion, and the O–Cl–O bond angles vary from 108.8 (6) to 110.1 (6)°. There are strong hydrogen bonding interactions involving the perchlorate ion.

Magnetic Susceptibility. Compound (1). A plot of χ_M^{corr} vs. temperature for solid $[Cu_2(OH)(ClO_4) \subset A](ClO_4)_2 \cdot CHCl_3$ is shown in Figure 6. Observed and calculated susceptibilities and magnetic moments are available in Table S8. The compound is almost completely diamagnetic at room temperature. The χ vs. T plot shows a slight rise, just above the noise level, in susceptibility with increasing temperature. The system is therefore very strongly antiferromagnetically coupled. The expected maximum in the magnetic susceptibility must occur well above the room temperature. Least-squares analysisof the data gave a spin-exchange coupling constant, J, of −496 (7) cm^{-1}, for the Hamiltonian $H' = -2J\bar{S}_1 \cdot \bar{S}_2$. With such a large coupling constant and no data even close to the maximum of the susceptibility, the results cannot be fit as well as, for example, those for the imidazolate-bridged compounds, which have $J \sim -26$ cm^{-1}.[2,3] This feature accounts for the large error in J. With the copper atoms having square-planar geometry, the unpaired electron is in the $d_{x^2-y^2}$ orbital. The bridging hydroxide ion, being in an equatorial position, is thus

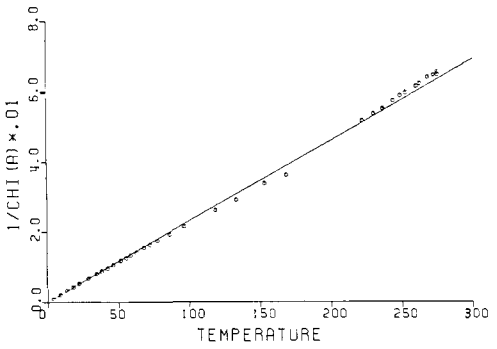

Figure 7. Plot of the inverse corrected atomic (per copper ion) magnetic susceptibility in cgs units of $[Cu_2(OAc)_2A]_n(ClO_4)_{2n}$ as a function of temperature in K. The open circles are the experimental data points, and the solid line is the result of the least-squares fitting of the parameters of a Curie–Weiss law to the data above 5 K.

well-placed to mediate the superexchange pathway. The bridging perchlorate ion, being only weakly coordinated to orbitals almost orthogonal to the one in which the unpaired electron resides, is very unlikely to contribute to the exchange.

In a series of dihydroxo-bridged dicopper(II) compounds, where the bridging oxygen atoms are in the equatorial planes of the copper ions, magnetic exchange is a function of the Cu–O–Cu angle.[15,19,31] The relationship $J = (X - 97.6°)(-37.3\ cm^{-1}/deg)$, X = Cu–O–Cu angle in degrees, fit the dihydroxo-bridged compounds quite well. The Cu–O–Cu angle in compound **1** is far outside the range, $X = 95–104°$, for which this relationship was developed. Extended to the present compound, the relationship predicts $J = -1716\ cm^{-1}$. If one hydroxide bridge is only half as good as two hydroxide bridges for determining the magnitude of the superexchange, then J should be $-858\ cm^{-1}$, which is still more than 70% greater than the observed value.

Other monohydroxo-bridged compounds in which the hydroxide ion lies in the basal plane of a distorted square-pyramidal geometry exhibit very strong magnetic exchange interactions.[7] Corresponding Cu–OH–Cu angles and J values are 141.7° and $-120\ cm^{-1}$; 132.2° and $-410\ cm^{-1}$; 110.3° and $-32\ cm^{-1}$. Except for the first of these, the trend parallels that seen for the dihydroxo-bridged compounds. Perhaps the dihedral angle between the two copper coordination planes linked by a single hydroxide bridge is an important factor in determining the magnitude of J. In compound **1** the perchlorate axial bridge holds this angle at a specific value which differs from that in $[Cu_2L(OH)]^{3+}$, where L is a 30-membered "N_6O_4" macrocyclic Schiff base ligand.[7d] Both these compounds have Cu–OH–Cu angles of ~141–143° but quite different J values of -497 and $-120\ cm^{-1}$, respectively. Further studies of monohydroxo-bridged dicopper(II) complexes will be of value.

Compound 2. A plot of $(\chi_M^{corr})^{-1}$ vs. T for polymeric $[Cu_2(OAc)A_2]_n(ClO_4)_{2n}$ is given in Figure 7. The data are well fit by a Curie–Weiss law; least-squares refinement to the expression $\chi_M^{corr} = C/(T - \theta)$ gave (solid line, Figure 7) $C = 0.435$ (2) and $\theta = -0.70$ (7)°. Observed and calculated values for χ_M^{corr} and μ_B are given in Table S9. Since $C = Ng^2\beta^2/4K$, the corresponding g value is 2.15, which is typical for copper(II). From the very small negative value of θ it can be estimated that the compound is slightly antiferromagnetic, with $J \sim -1\ cm^{-1}$.[32]

Compound **2** is a polymer. Since copper ions in the same macrocycle are linked only by the bis(2-aminoethyl) ether chains, magnetic interactions will be mediated primarily through the acetate bridges. In copper acetate and related carboxylate-bridged compounds there is a strong antiferromagnetic interaction.[25] As is obvious from the results of the susceptibility measurements, the interaction in compound **2** is much weaker. The difference in the strength of the magnetic coupling is due to two geometric features of the bridge. In copper acetate the bridges are in a syn–syn configuration, bringing the copper ions to within 2.64 Å of one another.[24] This short distance has led to arguments as to whether the exchange interaction is direct or through the bridging ligands.[33] In compound **2** the copper ions are bound in a syn–anti configuration with a copper–copper distance that is too long for a direct interaction. As mentioned above, several copper complexes have this geometry and their magnetic properties have been well studied, as shown in Table VI. The results are remarkably consistent, in spite of the different bridging ligands, and differ from those for both copper acetate and the present compound, **2**.

Table VI. Exchange Coupling Constants for Some Carbonate- and Carboxylate-Bridged Copper(II) Complexes

complex	bridge conformation	J, cm^{-1}	ref
$[Cu(OAc)(H_2O)]_2$	syn–syn	−150	25b
$[Cu(OAc)_2A]_n^{2n+}$	syn–anti	~−1	*a*
$[Cu(pip)(H_2O)]_3CO_3(NO_3)_4$	syn–anti	4.82 (4)	28
$Na_2Cu(CO_3)_2$	syn–anti	4.1 (7)	*b*
$Cu(OCH_2COO)_2 \cdot {}^1/_2H_2O$	syn–anti	4.66	26, *c*
$Cu(HCOO)_2$	syn–anti	6.88	27, 35

[a] This work. [b] Gregson, A. K.; Healy, P. C. *Inorg. Chem.* 1978, *17*, 2969. [c] Corvan, P. J.; Estes, W. E.; Weller, R. R.; Hatfield, W. E. *Inorg. Chem.* 1980, *19*, 1297.

The ferromagnetic interactions ($J \sim 4–7\ cm^{-1}$, Table VI) observed for the syn–anti bridged compounds differ from the very weak antiferromagnetic coupling interaction seen in compound **2** because of the second important structural feature. In this series of ferromagnetically coupled compounds, the bridging ligand is strongly bound to both copper ions through the orbital containing the unpaired electron. This geometry is very good for promoting magnetic exchange interactions. In compound **2**, the two bridging acetate groups form a link from a strongly bonding basal position, at which is directed the $d_{x^2-y^2}$ orbital that contains the unpaired electon, to a weakly bonding axial position, which is almost orthogonal to the other $d_{x^2-y^2}$ orbital. Thus even though there are two acetate bridges, there is no suitable pathway for strong magnetic interaction.

A similar effect has been previously observed for biimidazolate-bridged compounds.[34] The imidazolate ring of the bridging biimidazolate ligand bridged from an axial position on one copper ion to a basal position on another. This geometry was found not to provide a good pathway for magnetic exchange.

Although the foregoing geometric arguments explain the difference in the strength of the interaction in **2** compared to the other syn–anti bridged complexes, they may not explain the difference in the sign. Since the interaction is so weak, this difference may be unimportant. Nevertheless, there is an explanation for the sign change if the spin polarization model for superexchange[35] is to be believed. In this model, when one of the bonds in the exchange pathway is altered from one orbital to an orbital orthogonal to it, the sign of the interaction changes. This change is exactly what happens when comparing compound **2** with the series of syn–anti bridged compounds having ferromagnetic interactions.

Solution Stability of $[Cu_2(OH)\subset A]^{3+}$. While extensive tests of the viability of the hydroxide bridge in solution have not been carried out by us, the pH of the aqueous solution of the complex is 7.0, indicating that the bridge remains intact at neutral pH. The visible band, which has a λ_{max} at 637 nm, is preserved for $6 < pH < 11$, indicating that the bridge is stable over this range. This conclusion is strongly supported by potentiometric titration

(31) Crawford, V. H.; Richardson, H. W.; Wasson, J. R.; Hodgson, D. J.; Hatfield, W. E. *Inorg. Chem.* **1976**, *15*, 2107.
(32) Drago, R. S. "Physical Methods in Chemistry"; Saunders: Philadelphia, 1977, Chapter 11.
(33) (a) Doedens, R. J. *Prog. Inorg. Chem.* **1976**, *21*, 209. (b) Kato, M.; Jonassen, H. B.; Fanning, J. C. *Chem. Rev.* **1964**, *64*, 99.
(34) Haddad, M. S.; Duesler, E. N.; Hendrickson, D. N. *Inorg. Chem.* **1979**, *18*, 141.
(35) Inoue, M.; Kubo, M. *Inorg. Chem.* **1970**, *9*, 2310.

studies recently carried out by Martell.[5]

A shoulder at 330 nm in the optical spectrum appears to depend upon the perchlorate ion concentration. Upon initial dissolution of the compound in water, this band was very intense (ϵ 1800 M^{-1} cm^{-1}). After a few hours of standing in solution, the shoulder had disappeared. Addition of excess solid sodium perchlorate regenerated the shoulder. It is unusual to think of copper(II) as having slow, kinetically controlled processes, but such seems to be the case here. The simplest explanation is that the band is associated with a charge transfer that can only take place if perchlorate is also bridging two copper ions in the axial positions. Whether this charge transfer actually involves the perchlorate ion or depends upon the dihedral angle of the two copper coordination planes as influenced by the bridging perchlorate is unknown and worthy of further study.

Comparison with Binuclear Copper in Biology. The suggestion that the bridging unit linking two copper centers in biology might be oxide or phenoxide was made before there were any good models to support it.[36] Because of the inability of Cu(II) to accept π bonds from the oxide ion, it is likely that oxo-bridged dicopper(II) centers will not be very stable. The Cu–Cu distance in the present compound is very similar to the Cu–Cu distance estimated by EXAFS spectroscopy for the oxy form of the protein.[37] The magnetic interaction through the hydroxide bridge of compound **1**, while weaker than the estimated lower limit of the interaction in the protein,[38] suggests that hydroxide could mediate such a large magnetic exchange. Phenoxide should be similar in its ability to act as a superexchange pathway, as model studies have suggested.[18] With the number of monohydroxo-bridged dicopper(II) structures that have been found recently, and the data that indicate the Cu–OH–Cu unit to be fairly robust, hydroxide ion must also be considered as a likely candidate for the so-called "endogenous" bridging ligand for binuclear copper centers in biology.

Conclusions

In the presence of base, the dicopper(II) form of the binucleating macrocycle A readily forms the (μ-hydroxo)dicopper(II) complex, $[Cu_2(OH)\subset A]^{3+}$. The structure of the derivative in which perchlorate ion forms an additional weak bridge across the apical positions of the two square-pyramidal copper(II) centers has a wide Cu–OH–Cu angle and short Cu–O bonds. This geometry promotes strong antiferromagnetic coupling, making this complex one of the better available models for binuclear copper centers in biology. The structure of the crystalline acetate compound, $[Cu_2(OAc)_2A]_n(ClO_4)_{2n}$, demonstrates that we do not yet know all the rules that dictate whether a bridged bimetallic center will reside within a binucleating ligand or, as in this case, link an inverted form of the ligand in a polymeric array. At least three conformations, "planar", "U-shaped", and "S-shaped", of ligand A have been identified, and others are conceivable. The acetate-bridged dicopper(II) compound is of additional interest and importance because its syn–anti bridged structure has unique magnetic properties. Unlike syn–syn copper acetate the magnetic coupling between the copper ions is very weak, and because the acetate ion bridges apical and equatorial sites, the interaction is antiferromagnetic rather than ferromagnetic. In basic solutions the acetate and carbonate derivatives of $\{Cu_2\subset A\}^{4+}$ revert to $[Cu_2(OH)\subset A]^{3+}$, suggesting that in biological systems at neutral pH there will be a strong tendency to form this unit if permitted by the protein conformation and accessibility to solvent.

Acknowledgment. This work was supported by National Institutes of Health Research Grants GM-16449 (at Columbia) and GM-32134 (at MIT) and by the National Science Foundation Grants CHE-82-19587 (at Columbia) and CHE-83-40769 (at MIT). We thank Prof. J.-M. Lehn for a generous supply of ligand A and Dr. G. Kolks for helpful discussions.

Supplementary Material Available: Hydrogen atom positional parameters, thermal parameters for all atoms, observed and calculated structure factors for **1** and **2**, torsion angles for the ligand in $[Cu_2(im)(imH)_2\subset A](ClO_4)_3$ and **1** and **2**, and observed and calculated magnetic susceptibilities and moments for **1** and **2** (39 pages). Ordering information is given on any current masthead page.

(36) Eichman, N. C.; Himmelwright, R. S.; Solomon, E. I. *Proc. Natl. Acad. Sci. U.S.A.* **1979**, *76*, 2094.

(37) (a) Co, M. S.; Scott, R. A.; Hodgson, K. O. *J. Am. Chem. Soc.* **1981**, *103*, 984. (b) Brown, J. M.; Powers, L.; Kincaid, B.; Larrabee, J. A.; Spiro, T. G. *Ibid.* **1980**, *102*, 4210.

(38) (a) Moss, T. H.; Gould, D. C.; Ehrenberg, A.; Loehr, J. S.; Mason, H. S. *Biochemistry* **1973**, *12*, 1244. (b) Solomon, E. I.; Dooley, D. M.; Wang, R. H.; Gray, H. B.; Cerdonio, M.; Mogno, F.; Romaine, G. L. *J. Am. Chem. Soc.* **1976**, *98*, 1029. (c) Dooley, D. M.; Scott, R. A.; Ellinghaus, J.; Solomon, E. I.; Gray, H. B. *Proc. Natl. Acad. Sci. U.S.A.* **1978**, *75*, 3019.